Title

Derivation of functional trophoblast stem cells from primed human pluripotent stem cells

Journal

Stem Cell Reports, 17(6)

ISSN

2213-6711

Authors

Soncin, Francesca

Morey, Robert

Bui, Tony

et al.

Publication Date

2022-06-01

DOI

10.1016/j.stemcr.2022.04.013

Peer reviewed

Stem Cell Reports
Article

ISSCR

OPEN ACCESS

Derivation of functional trophoblast stem cells from primed human pluripotent stem cells

Francesca Soncin,[1,2,4] Robert Morey,[2,3,4] Tony Bui,[1,2] Daniela F. Requena,[1,2] Virginia Chu Cheung,[1,2,3] Sampada Kallol,[1,2] Ryan Kittle,[1,2] Madeline G. Jackson,[1,2] Omar Farah,[1,2] Jennifer Dumdie,[1,2] Morgan Meads,[1,2] Donald Pizzo,[1] Mariko Horii,[1,2] Kathleen M. Fisch,[3] and Mana M. Parast[1,2,*]

[1]Department of Pathology, University of California San Diego, La Jolla, CA 92093, USA
[2]Sanford Consortium for Regenerative Medicine, University of California San Diego, La Jolla, CA 92093, USA
[3]Department of Obstetrics, Gynecology, and Reproductive Sciences, University of California San Diego, La Jolla, CA 92093, USA
[4]These authors contributed equally
*Correspondence: mparast@ucsd.edu
https://doi.org/10.1016/j.stemcr.2022.04.013

SUMMARY

Trophoblast stem cells (TSCs) have recently been derived from human embryos and early-first-trimester placenta; however, aside from ethical challenges, the unknown disease potential of these cells limits their scientific utility. We have previously established a bone morphogetic protein 4 (BMP4)-based two-step protocol for differentiation of primed human pluripotent stem cells (hPSCs) into functional trophoblasts; however, those trophoblasts could not be maintained in a self-renewing TSC-like state. Here, we use the first step from this protocol, followed by a switch to newly developed TSC medium, to derive bona fide TSCs. We show that these cells resemble placenta- and naive hPSC-derived TSCs, based on their transcriptome as well as their *in vitro* and *in vivo* differentiation potential. We conclude that primed hPSCs can be used to generate functional TSCs through a simple protocol, which can be applied to a widely available set of existing hPSCs, including induced pluripotent stem cells, derived from patients with known birth outcomes.

INTRODUCTION

The human placenta is a unique transient organ that is responsible for proper growth and development of the fetus *in utero* (Burton and Jauniaux, 2015). The epithelial cells in the placenta arise from trophectoderm (TE), the first lineage to segregate during embryonic development (Niakan et al., 2012). Much of what we know about trophoblast lineage specification and early placental development comes from studies in rodents; however, numerous studies using human embryos and early-gestation placental tissues over the past few years have highlighted multiple key differences in these processes in human (Blakeley et al., 2015; Soncin et al., 2015, 2018). These include a later specification of TE in the human embryo and altered/lack of expression of genes, such as *EOMES*, which are key to mouse TE establishment and expansion (Blakeley et al., 2015; Soncin et al., 2018). As a result of these differences, culture conditions for the derivation of mouse trophoblast stem cells (TSCs), established over 20 years ago (Tanaka et al., 1998), do not give rise to similar cells when applied to human embryos or placental tissues (Kunath et al., 2014).

Recently, distinct culture conditions for the derivation and maintenance of human TSCs were established and include epidermal growth factor (EGF), as well as inhibitors of tumor growth factor beta (TGF-B) and GSK3B (Okae et al., 2018). Variations of this protocol were reported shortly thereafter for the establishment of self-renewing trophoblast organoids (Haider et al., 2018; Turco et al., 2018). Nevertheless, these protocols are only able to establish such cells or organoids from early-first-trimester (<10 week gestational age) human placental tissues and could not be applied to placental tissues at term. This limits the utility of these cells, as, aside from the ethical challenges of using such tissues, the disease potential of these cells is mostly unknown, necessitating development of other model systems from tissues with known pregnancy outcomes.

We previously developed a two-step protocol for the differentiation of primed human pluripotent stem cells (hPSCs) into terminally differentiated, functional trophoblast and demonstrated its use in modeling human trophoblast differentiation in the setting of both normal development and disease (Horii et al., 2016). This protocol uses bone morphogenetic protein-4 (BMP4), which is also known to induce mesoderm in a WNT-dependent manner (Kurek et al., 2015). As such, we recently updated this protocol, applying the WNT inhibitor IWP2 to the first step, which directs differentiation solely toward the trophoblast lineage (Horii et al., 2019). However, while this protocol produced cells resembling cytotrophoblast (CTB), the proliferative stem cell population in the placenta from which TSCs are derived, these cells could not be maintained in a self-renewing state.

Here, we have applied a culture medium, recently developed for maintenance of induced TSCs (iTSCs), reprogrammed from term CTB (Bai et al., 2021) to hPSC-derived CTB, and show that this transitions the cells into bona

fide TSCs. These cells resemble placenta-derived TSCs and can be differentiated into functional syncytiotrophoblast (STBs) and extravillous trophoblast (EVTs), both *in vitro* and *in vivo*. In addition, we compare these cells with those recently derived from naive hPSCs (Io et al., 2021) and show that they resemble naive hPSC-derived TSCs, both during the transition from pluripotency to TE and in the final CTB-like state. We conclude that, similar to their naive counterparts, primed hPSCs can be converted to self-renewing TSCs following a short induction period with BMP4-containing media.

RESULTS

Generation of TSC-like cells from primed hPSCs

We previously developed a two-step protocol for trophoblast differentiation of primed hPSCs (Horii et al., 2019). This protocol involved an initial induction of cells resembling villous CTB, uniformly expressing *TP63*, using a combination of BMP4 and the WNT inhibitor IWP2. This led to the formation of a uniform group of EGFR$^+$ CTB stem-like cells, which, though not able to self-renew, could be further differentiated, using BMP4 in the presence of feeder-conditioned media, into a mixed set of terminally differentiated trophoblasts, including multinucleated human chorionic gonadotropin (hCG)-secreting STBs and invasive surface HLA-G$^+$ EVTs. Nevertheless, this was not only a heterogeneous mixture of trophoblast but also tended to favor STB formation, with only a minority (10%–20%) of EVTs in the final culture. Here, we applied a new medium to CTB stem-like cells at the end of step 1 of our trophoblast differentiation protocol (Figure 1A). This medium was developed originally by the Kessler lab for the reprogramming of term CTB into TSC-like cells (iTSCs) (Bai et al., 2021) and is a modification of the Okae medium (see experimental procedures) used for derivation of TSCs from human embryos and early-gestation placentae (Okae et al., 2018). After passage in this medium at least 5 times, we were able to derive cells morphologically resembling primary TSCs (Figure 1B) and uniformly expressing cell-surface TSC markers EGFR and ITGA6 (Figure 1C). Similar to primary TSCs (Figure S1A), the hPSC-derived TSCs uniformly expressed GATA3 and KRT7 (Figure 1D). We successfully derived such cells from both human embryonic stem cell (hESC) lines (WA09/H9 and WA01/H1) and induced PSCs (iPSCs) (Figure S1B), having been able to keep these cells in culture for over 20 passages.

Characterization of cellular identity of hPSC-derived TSCs

We next moved to compare the transcriptome of these cells with primary TSCs, which we recently derived from early-gestation placental tissues in our own laboratory (Morey et al., 2021), and have confirmed their identity by direct comparison with the Okae cells (Okae et al., 2018). We isolated RNA from the hPSCs in both the undifferentiated state and at days 1–4 post trophoblast induction, as well as from hPSC-derived TSCs and the two primary TSC lines (1048 and 1049). Principal-component analysis (PCA) and K-means clustering separated these samples into three groups, with undifferentiated hPSCs and hPSCs treated with BMP4-IWP2 for 1 day into one, hPSCs treated with BMP4/IWP2 (days 2–4) into a second, and primary and hPSC-derived TSC samples into a third cluster (Figure 2A); increasing K did not further separate the samples in a biologically meaningful manner (data not shown). The transcriptomes of primary TSCs and undifferentiated hPSCs were then directly compared (variance = 0.05, two-group analysis $q < 0.05$), leading to the identification of 1,618 differentially expressed genes, of which 839 genes were upregulated in TSCs and 779 in PSCs (Figure 2B; Data S1). We performed gene set enrichment analysis (GSEA) and found hPSC-derived TSCs were enriched in genes highly expressed in placenta-derived hTSCs (adjusted p value [padj] < 0.004, enrichment score [ES] = 0.44, and normalized ES [NES] = 2.44) compared with hPSCs. We validated expression levels of a handful of TSC-associated markers (*TP63*, *VGLL1*, *ELF5*, *ITGA6*, and *EGFR*) by qPCR and found that the hPSC-derived TSCs expressed most of these markers at similar levels to primary hTSCs (Figure 2C). Similar to primary TSCs, hPSC-derived TSCs showed uniform expression of TSC markers, including *TP63* and *CDH1*, and a lack of pluripotency marker *POU5F1/OCT4* (Figure S2A). We have previously reported co-expression of *CDX2* and *TP63* in hPSCs following 4 days of BMP4 treatment (Horii et al., 2016), while Okae et al. (2018) have reported low/variable levels of *CDX2* expression in primary TSCs. We noted that, compared with primary TSCs, hPSC-derived TSCs showed similar *CDX2* levels by qPCR (Figure 2C) and a similarly variable nuclear expression of this protein by immunofluorescence (Figure S2B).

Primary TSCs can only be derived from early-first-trimester (<10 week gestational age) CTB (Okae et al., 2018). We therefore asked how both our primary and hPSC-derived TSCs compared with CTB isolated from early- (6–8 weeks, CTB_1E) versus late- (10–14 weeks, CTB_1L) first-trimester placentae. Transcriptomic analysis showed that both primary and hPSC-derived TSCs were distinct from isolated CTB (Figure S2C). Unsupervised hierarchical clustering was performed with primary CTB sub-groups combined and independently. The group of samples including both primary and hPSC-derived TSCs joined the branch with early-first-trimester CTB when these cells were included in the analysis, while they joined the branch with undifferentiated and BMP-treated hPSCs when

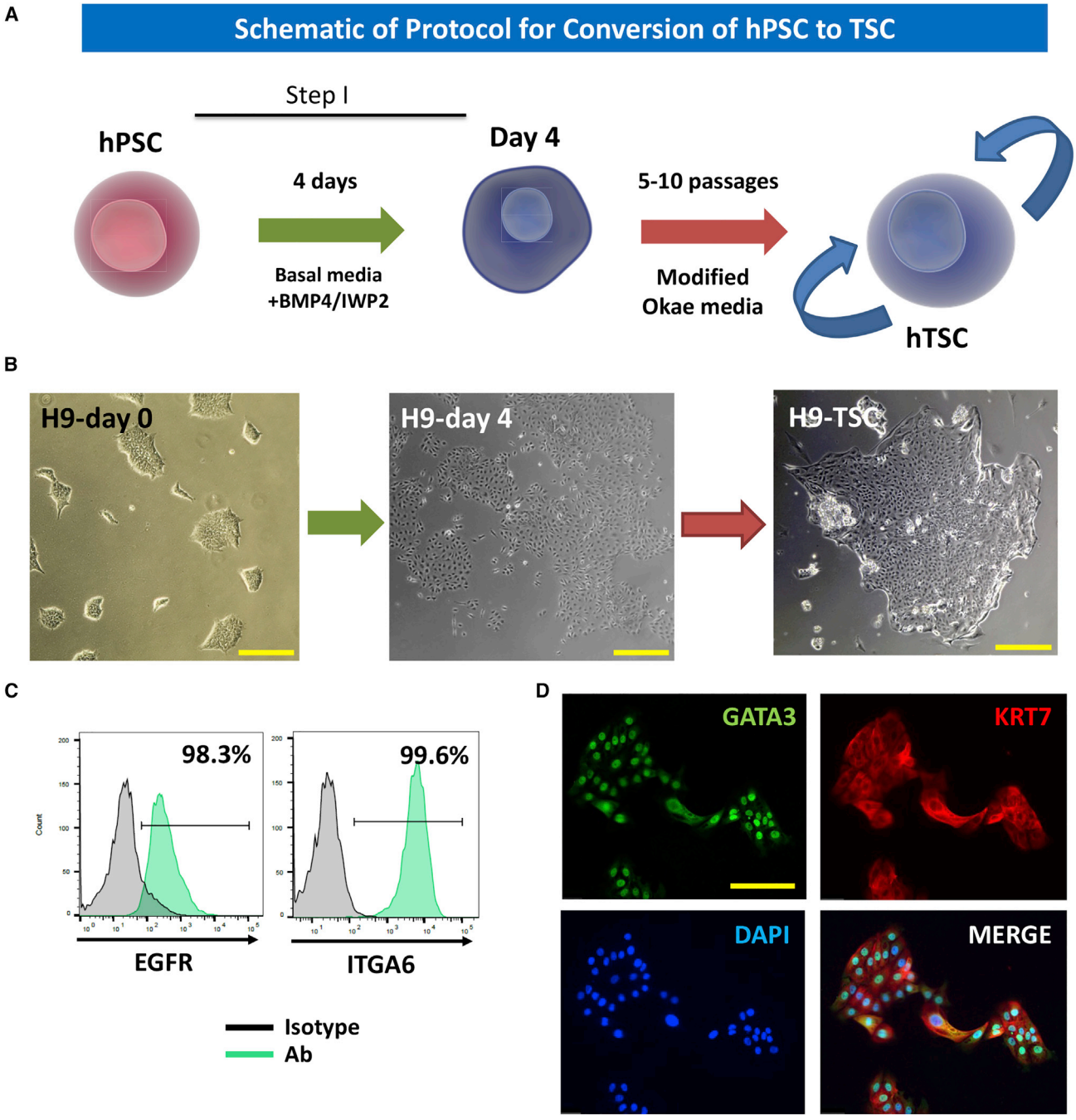

Figure 1. Protocol for conversion of primed hPSCs into TSCs

(A) Protocol schematic.

(B) Morphology of H9 hESC line as undifferentiated (day 0), following 4 days of BMP4/IWP2 treatment (day 4), and after 5 passages in our modified Okae medium for TSCs (H9-TSCs). Bar: 312.5 μm.

(C) Flow-cytometric analysis of H9-derived TSCs for EGFR and ITGA6.

(D) Immunofluorescence staining of H9-TSCs for GATA3 and KRT7. Bar: 124.5 μm.

Data in (B–D) are representative of n = 5 independent experiments.

See also Figure S1.

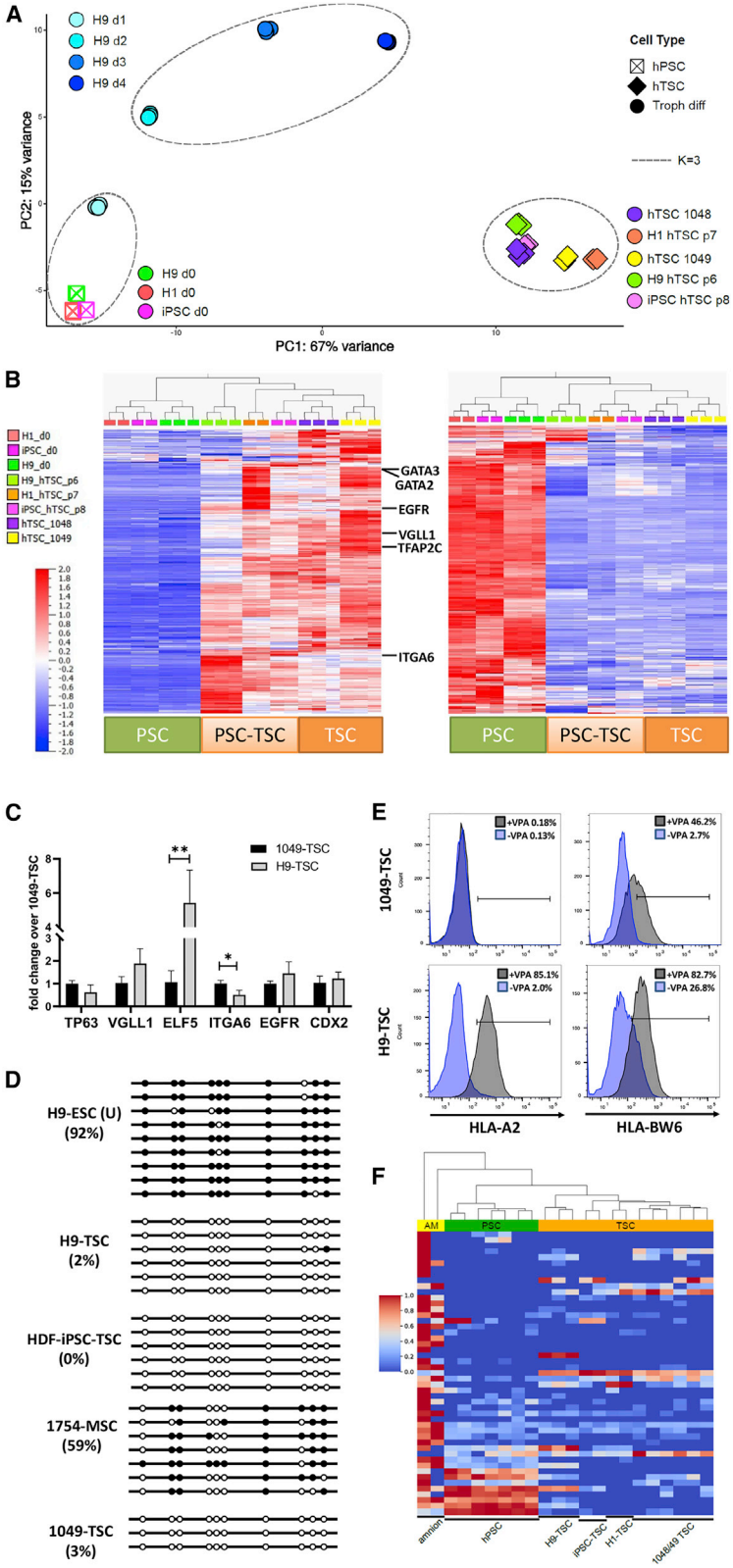

Figure 2. Characterization of hPSC-derived TSCs

(A) Principal-component analysis of hPSCs (undifferentiated/day 0), H9 hESCs treated with BMP4/IWP2 for 1–4 days, hPSC-derived TSCs after 6–8 passages in the modified Okae TSC medium (TSC), and primary (placenta-derived) TSCs (lines 1048 and 1049). Each dot on the principal-component analysis (PCA) represents a sample from an independent experiment (n = 2 for H1 and iPSCs, day 0 and TSC; n = 3 for all other samples). Sample clusters from k-means clustering, marked by circles, show that hPSC-derived TSCs cluster together with primary (placenta-derived) hTSCs.

(B) Heatmaps of undifferentiated hPSCs and primary and hPSC-derived TSCs showing genes that are either upregulated (839 genes) or downregulated (779 genes) in primary TSCs compared with undifferentiated hPSCs. GSEA shows that hPSC-derived TSCs were enriched in primary TSC-associated genes (NES 2.44, padj < 0.004) but not in (undifferentiated) hPSC-associated genes. A few TSC-associated genes are noted in the heatmap.

(C) qPCR of the indicated CTB markers in undifferentiated primary TSC (1049) compared with hPSC (H9)-TSCs. Data were normalized to *L19* and shown as fold change over undifferentiated 1049 (D0 = day 0) and represent mean ± SD for n = 3 independent experiments. *p < 0.05; **p < 0.01 by Student's t test.

(D) DNA methylation surrounding the *ELF5* promoter in undifferentiated (U) H9 ESCs, TSCs derived from both H9 and a human dermal fibroblast (HDF)-derived iPSCs, an umbilical-cord-derived mesenchymal stem cell line (1754), and a primary (placenta-derived) TSC line (1049). Each line represents a distinct sequenced clone (n = 3 to 9).

(E) Flow-cytometric analysis of primary (1049) and hPSC (H9)-derived TSCs for HLA-A2 and HLA-Bw6 with (gray) and without (purple) valproic acid (VPA) in the culture medium. Data are representative of 2 independent experiments.

(F) Heatmap of amnion-specific markers (based on a more stringent analysis by Seetheram et al. in this issue of *Stem Cell Reports* of the Roost et al., 2015 dataset) in undifferentiated hPSCs and primary (1048 and 1049 TSC) and hPSC-derived TSCs, as well as amnion (AM). GSEA showed that neither primary nor hPSC-derived TSCs were enriched in amnion-specific genes (NES = -0.94 with padj = 0.561 and NES = -1.06 with padj = 0.354, respectively).

See also Figure S2.

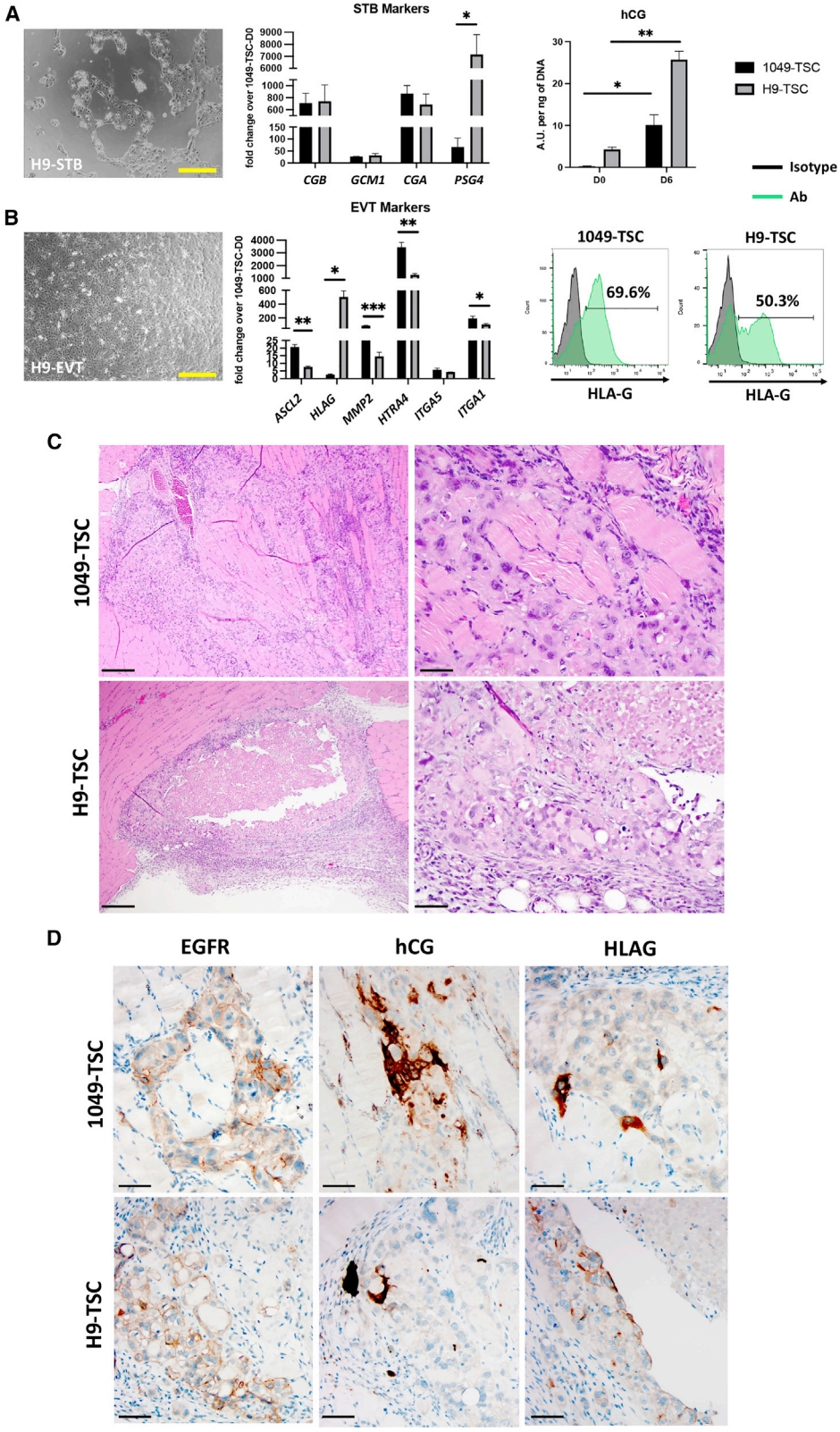

(legend on next page)

compared with the late-first-trimester CTB group only (compare left and center dendrograms with the one on the right in Figure S2D).

We next aimed to go beyond the transcriptome and characterize three other features of early-gestation CTB in our hPSC-derived TSCs, namely the methylation status of the *ELF5* promoter, the expression of class I human leukocyte antigens (HLAs), and the expression of the C19 microRNA (miRNA) cluster. The *ELF5* promoter is known to be hypermethylated in hPSCs but hypomethylated in early-gestation CTB (Hemberger et al., 2010) and primary TSCs (Okae et al., 2018). Compared with both undifferentiated hPSCs and mesenchymal stem cells derived from umbilical cord (Horii et al., 2021), both primary and hPSC-derived TSCs showed significant hypomethylation of this genomic region (Figure 2D). In addition to a hypomethylated *ELF5* promoter, villous CTB and TSCs, which are thought to reside within the CTB layer, are both known to lack expression of class I HLAs (HLA-A and HLA-B) (Apps et al., 2009; Io et al., 2021). When we evaluated our cells by flow cytometry, both primary and hPSC-derived TSCs expressed class I HLAs. Therefore, we re-evaluated our media components and noted that valproic acid (VPA), a histone deacetylase (HDAC) inhibitor, had been previously identified as a compound that promotes class I HLA expression in tumor cells (Armeanu et al., 2005; Mora-García et al., 2006; Yamanegi et al., 2010; Yang et al., 2020). When we removed this chemical from our medium, after only three passages, class I HLA expression significantly decreased in both primary and hPSC-derived TSCs (Figure 2E), without affecting self-renewal. A third feature of human trophoblast is high expression of the primate-specific, maternally imprinted C19 miRNA cluster (Donker et al., 2012; Noguer-Dance et al., 2010). We evaluated the expression of four members of this miRNA cluster and found that while hPSC-derived TSCs upregulated one (MIR526b-3p) compared with undifferentiated hPSCs, overall, none reached the levels seen in primary TSCs and JEG3 choriocarcinoma cells (Figure S2E).

It has been argued that, unlike naive hPSCs, primed hPSCs give rise to amnion when treated with media containing BMP4 (Guo et al., 2021; Io et al., 2021). To further examine the identity of hPSC-derived TSCs, we next evaluated the expression of a set of amnion-specific genes in primary TSCs compared with hPSCs and their TSC derivatives. We first used an amnion-specific gene list originally published by Roost et al. (2015): GSEA showed that primary TSCs were negatively enriched (NES = -2.18 and padj < 0.0005), while hPSC-derived TSCs were also not enriched (NES = -1.16 and padj = 0.132), for amnion genes. Subsequently, we performed GSEA using an amnion gene list obtained through a more stringent analysis of the one by Roost et al. (2015), as performed by Seetheram et al. (2022) (Figure 2F). In this GSEA analyses, neither primary nor hPSC-derived TSCs were enriched in amnion-specific genes (NES = -0.94 with padj = 0.561 and NES = -1.06 with padj = 0.354). Based on these data, as well as the many shared features with primary TSCs, we conclude that we have successfully derived TSC-like cells from primed hPSCs.

Functional characterization of hPSC-derived TSCs

We next moved to characterize the differentiation ability of primed hPSC-derived TSCs. When differentiated into STBs, they upregulated appropriate markers, including *CGA*, *CGB*, *GCM1*, and *PSG4*, by qPCR and secreted hCG into the medium at similar levels as primary TSC-derived STBs (Figure 3A). Similarly, hPSC-derived TSCs could be differentiated into EVTs, expressing similar levels of EVT markers, including *ASCL2*, *HLAG*, *MMP2*, *HTRA4*, *ITGA5*, and *ITGA1*, and gaining surface HLA-G expression, similar to primary TSC-derived EVTs (Figure 3B). Finally, when injected into NOD-SCID mice, both primary and hPSC-derived TSCs produced mixed trophoblastic tumors composed of both hCG^+ and $HLA\text{-}G^+$ cells (Figures 3C and 3D). Thus, both *in vitro* and *in vivo*, hPSC-derived TSCs showed the capacity to

Figure 3. *In vitro* and *in vivo* differentiation potential of hPSC-derived TSC

(A) Morphology, lineage-specific gene expression, and hCG secretion of primary (1049) and hPSC (H9)-derived TSCs differentiated into syncytiotrophoblast (STB). Bar: 312.5 μm. qPCR data were normalized to L19 and shown as fold change over undifferentiated (day 0/D0) 1049 TSCs. hCG secretion was normalized to ng of DNA. Both qPCR and ELISA data represent mean ± SD for n = 3 independent experiments. *p < 0.05; **p < 0.01 by Student's t test.

(B) Morphology, lineage-specific gene expression, and flow-cytometric analysis for surface HLA-G expression of primary (1049) and hPSC (H9)-derived TSCs differentiated into extravillous trophoblast (EVT). Bar: 312.5 μm. qPCR data were normalized to *L19* and shown as fold change over undifferentiated (day 0/D0) 1049 TSCs and represent mean ± SD for n = 3 independent experiments. *p < 0.05; **p < 0.01; ***p < 0.001 by Student's t test. Flow-cytometric data are representative of 3 independent experiments.

(C and D) Tumors generated 10 days following injection of primary (1049) and hPSC (H9)-derived TSCs into NOD-SCID mice (representative of n = 2 independent experiments). (C) H&E staining shows the tumor cells invading through muscle (1049-TSC tumor) or forming a tumor with a necrotic center (H9-TSC), both characteristic of human trophoblastic tumors. Scale bars: 250 μm for low-power (left) and 50 μm for high-power (right) images. (D) Immunohistochemical staining of the same tumors using antibodies against EGFR, hCG, and HLAG shows positively stained cells (brown) in the TSC-derived lesions. Scale bars: 50 μm.

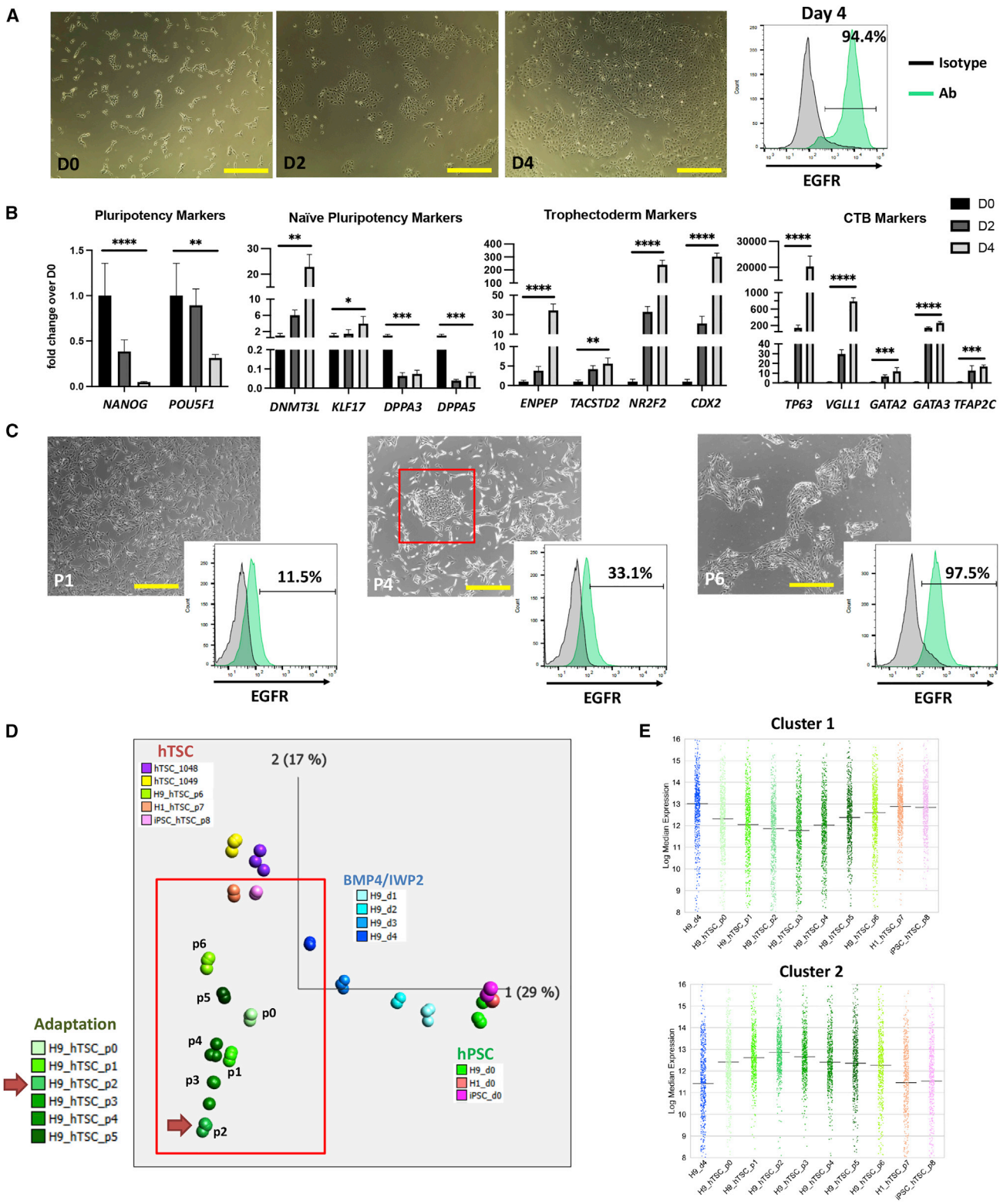

Figure 4. Transition from primed pluripotency to TSCs involves a trophectoderm-like intermediate

(A) Morphology of H9-ESCs at days 0, 2, and 4 following treatment with BMP4/IWP2. At the end of 4 days, over 94% of the cells express EGFR by flow-cytometric analysis. Data are representative of n = 5 independent experiments. Bar: 312.5 μm.

(legend continued on next page)

differentiate into both terminally differentiated trophoblast lineages.

Characterizing the path from primed pluripotency to TSCs

Our trophoblast induction protocol (Horii et al., 2019) was partially based on a previous study by Kurek et al. (2015), showing that BMP4 induces both trophoblast and mesoderm lineages, where only the latter lineage is WNT dependent. Thus, the addition of IWP2 should allow exclusive differentiation into trophoblast. We evaluated cells at the end of step 1 (BMP4/IWP2 treatment for 4 days) and noted the gradual flattening of the cells from pluripotency to this stage and a gain of EGFR expression (Figure 4A). By qPCR, these cells lost expression of pluripotency factors and gained expression of markers of TE, including *NR2F2* and *CDX2*, as well as markers of CTB, including *VGLL1* and *TP63* (Figure 4B); with the exception of *DNMT3L*, markers of naive pluripotency were either decreased or only slightly increased (Figure 4B). The transition from this state to TSCs through several rounds of passage in our modified Okae medium was characterized by an initial transition of cells into a mesenchymal morphology, with a loss of EGFR, and then a gradual re-epithelialization, with a re-gaining of EGFR (Figure 4C). Transcriptomic analysis of this adaptation phase showed unique changes in the gene expression of cells from passage 0 (p0) to p2, before returning back to a signature that more closely resembled primary TSCs (Figure 4D). Of the 839 genes differentially upregulated in primary TSCs compared with undifferentiated hPSCs, 37% (308 genes) were already upregulated at the end of step I, while 59% (492 genes) were upregulated in hPSC-derived TSCs (Figure S3A; Data S2). The adaptation did not change the nature of the cells, as the most significant tissue-specific signature of all the time points was associated with "placenta" (Figure S3B). Compared with cells at the end of step 1 (4 days of BMP4/IWP2 treatment), cells at p0 (about 48 h after being switched to TSC medium) demonstrated downregulation of genes associated with apical junction, apoptosis, G2-M checkpoint, and epithelial-mesenchymal transition (Data S2 and S3), which correlates with the observed morphology. We performed Click-clustering analysis of differentially expressed genes (DEGs) across the adaptation phase (Data S4), which revealed two main patterns of gene expression change (Figures 4E and S3C). Cluster 1 included 672 genes that showed an initial progressive downregulation, with the lowest expression at p2 of adaptation, followed by subsequent progressive upregulation through p6 (Figure 4E). Gene Ontology and pathway analysis revealed enrichment in terms associated with cell proliferation, apical junction, and various metabolic processes (Figure S3D). Cluster 2 contained 453 genes showing the converse pattern of expression, with a peak at p2 and subsequent downregulation through p6 (Figure 4E). Gene Ontology (GO) and pathway analysis showed enrichment in terms associated with epithelial-mesenchymal transition (EMT), which correlate with similarly noted changes in morphology, as well as apoptosis (Figure S3D). Taken together, these data show an adaptive response to hTSC media, involving the selection of a subset of cells (through apoptosis and subsequent proliferation) that undergo an EMT process to transition into the TSC state.

Recently, Io et al. (2021) developed a BMP4-based protocol for transitioning naive hPSCs first into a TE-like state (after 3 days), characterized by expression of *ENPEP*, *TACSTD2*, and *NR2F2*, and subsequently into a CTB-like state (after 3–15 passages), characterized by *SIGLEC6*, among other markers (including *VGLL1*, *TP63*, and *EGFR*). We compared our cells with theirs, starting with bulk RNA sequencing (RNA-seq), from primary CTB isolated by both our groups, as well as naive and primed hPSCs and their trophoblast derivatives. PCA showed separation between the naive and primed hPSC group and primary CTB (separated along the PC1 axis, 67% variance), with both the naive and primed hPSC-derived cells located

(B) qPCR of H9-ESCs at days 0, 2, and 4 following BMP4/IWP2 treatment, for markers of pluripotency (*NANOG* and *POU5F1*), naive pluripotency (*DNMT3L*, *KLF17*, *DPPA3*, and *DPPA5*), trophectoderm (*ENPEP*, *TACSTD2*, *NR2F2*, and *CDX2*), and cytotrophoblast (CTB) (*TP63*, *VGLL1*, *GATA2*, *GATA3*, *TFAP2C*). Data were normalized to *L19* and shown as fold change over undifferentiated H9-ESCs (D0 = day 0). *p < 0.05; **p < 0.01; ***p < 0.001; ****p < 0.0001 by Student's t test.

(C) Morphology and EGFR expression of BMP4/IWP2-treated H9-ESCs passaged in modified Okae TSC medium. During this time, the cells initially lose EGFR expression and slowly re-gain it after at least 5 passages. Data are representative of n = 3 independent experiments. Bar: 312.5 μm.

(D) PCA of cells transitioning from primed pluripotency (hPSCs) through BMP4/IWP2 induction then undergoing adaptation through 6 passages (p0–p6) in modified Okae TSC medium. Arrow points to the passage in which the hPSC-derived cells are farthest away from primary TSC. Each dot on the PCA represents a sample from an independent experiment (n = 2 for H1 and iPSC, day 0 and TSC; n = 3 for all H9 samples).

(E) Median expression of genes in clusters 1 and 2 from Click-clustering analysis Figures S3C and S3D) of H9-ESCs at day 4 of BMP4/IWP2 treatment and across TSC medium adaptation (10 sample groups indicated by red box in D).

See also Figure S3.

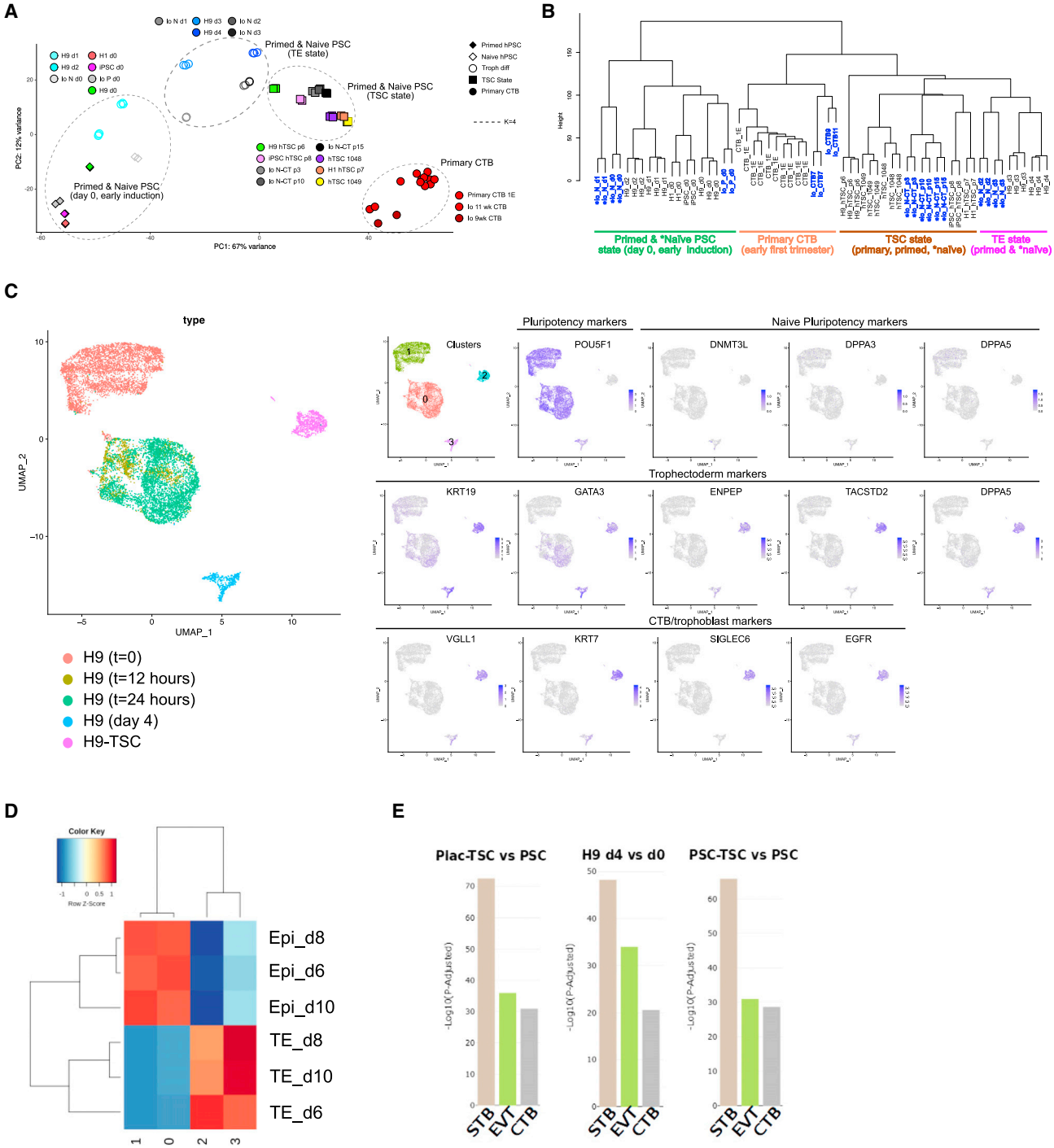

Figure 5. Comparison of trophectoderm and TSC derived from naive and primed hPSCs

(A) PCA of our cells, combined with those published by et al., 2021, including, from left to right, (1) undifferentiated naive and primed hPSCs (day 0) and their early trophoblast derivatives (days 1–2 in our BMP4/IWP2 treatment, and day 1 of Io et al.'s induction); (2) naive and primed hPSCs induced into a trophectoderm/TE-like fate (days 3–4 in our BMP4/IWP2 treatment, and days 2–3 of Io et al.'s induction); (3) primary (placenta-derived) TSCs (1048 and 1049 lines), our primed hPSC-derived TSCs (H9-TSCs at passage 6, H1-TSCs at passage 7, iPSC-TSCs at passage 8), and Io et al.'s naive hPSC-derived TSCs (naive cytotrophoblast [N-CT] at passages 3–15); and (4) primary CTB (CTB-1E include our preps from 10 different 5- to 8-week-gestation placentae; other four samples include two 9-week- and two 11-week-gestation CTB preps from Io et al., 2021). For hPSC lines, each dot represents a sample from an independent experiment

(legend continued on next page)

between these two groups on PC1 (Figure 5A). Unsupervised hierarchical clustering showed that while naive and primed hPSCs and their early derivatives (Io's naïve TE at day 1, and our BMP4/IWP2-treated cells at days 1–2) clustered together, all the later derivatives (Io's naïve TE at days 2–3, and our BMP4/IWP2-treated cells at days 3–4, as well as both naïve- and primed-hPSC-derived TSC) clustered together with primary CTB (Figure 5B). Within the latter group, our BMP4/IWP2-treated cells (at days 3–4) clustered together with Io's naïve TE (at days 2–3), suggesting that the primed cells go through a TE-like phase, while our primed TSCs (at passage 6–8) clustered together with Io's naïve CTB (at passage 3–15) (Figure 5B). Finally, integrating ours and Io's data with two other RNA-seq datasets (TSCs derived from primed hPSCs, by Wei et al. (2021), and iTSCs derived by capturing cellular intermediates during reprogramming of fibroblasts using TSC media, by Liu et al. [2020]) showed similar results (Figure S4). With k = 4, the cells clustered as follows: (1) all primary CTB (from first-trimester placenta); (2) all TSCs, irrespective of the cell of origin (primary, primed, or naive PSC-derived or directly reprogrammed iTSCs); (3) naive PSCs at day 0 and induced into TE (days 1–3) as well as BMP4/IWP2-treated primed PSC at days 3–4; and finally, (4) all primed PSCs as well as BMP4/IWP2-treated primed PSCs at days 1–2 (Figure S4). With an increase to k = 5, the third cluster (labeled "C" in Figure S4) broke into two, with the naive PSCs at days 0 and 1 of TE differentiation in one cluster and naïve TE at days 2–3 and BMP4-IWP2-treated primed PSCs at days 3–4 in the second cluster, again suggesting that the BMP4-IWP2-treated primed hPSCs undergo a TE-like phase. A further increase in k did not separate the samples in a biologically meaningful manner (data not shown).

We next evaluated the progression from primed pluripotency to TSCs by single-cell RNA-seq (scRNA-seq) of H9 hESCs, both undifferentiated and treated with BMP4/IWP2 for 12 h, 24 h, and 4 days, as well as H9-TSC, using 10X Genomics. A total of 11,259 cells across all time points were analyzed by Seurat, which separated the cells into 4 clusters (Figure 5C). Cluster 0, despite containing mostly cells at early stages of trophoblast induction with BMP4/IWP2 (12 and 24 h), showed a separate transcriptional program from undifferentiated hPSCs in cluster 1. Feature plots of pluripotency- and trophoblast-associated genes showed that both clusters 0 and 1 have a strong pluripotency signature (*POU5F1* and *NANOG*), with a subset of cluster 0 cells initiating the TE program, as noted by *GATA3* expression, as early as 12 h from induction. Cluster 3 cells (those treated with BMP4/IWP2 for 4 days) had completely lost *NANOG* expression but had begun to express TE-associated genes, including *KRT19*, *ENPEP*, *TACSTD2*, and *NR2F2*, similar to Io's naive PSC-derived TE (Io et al., 2021) (Figure 5C). As TSCs, cells gained expression of CTB-associated genes, including *EGFR*, *VGLL1*, and *SIGLEC6*, similar to Io's naive PSC-derived CTB (Io et al., 2021) (Figure 5C). Naive pluripotency markers were expressed at low levels in rare undifferentiated primed hPSCs, but (with the exception of *DNMT3L*) they were absent in BMP4/IWP2-treated hPSCs (Figure 5C). When we evaluated our scRNA-seq cell clusters using epiblast (EPI) and TE gene signatures obtained from day 6–10 extended-culture human embryos (Zhou et al., 2019) (Data S5), clusters 0 and 1 showed enrichment in EPI-specific genes, while clusters 2 and 3 showed enrichment in TE-specific genes (Figure 5D). Finally, when the transcriptomic signatures of hPSCs at day 4 of BMP4/IWP2 treatment as well as both primary and hPSC-derived TSCs were compared with undifferentiated hPSCs and analyzed by the PlacentaCellEnrich tool (Jain and Tuteja, 2021), all 3 groups showed the highest enrichment of genes from trophoblast cells in the placenta, with similar enrichment for STB-, EVT-, and CTB-associated genes (Figure 5E). These data suggest that primed hPSCs have the potential to give rise to TSCs following induction into a TE-like phase with 4 days of treatment with BMP4/IWP2, providing a simple

(n = 2 for H1 and iPSCs, day 0 and TSCs, and all samples from Io et al., 2021; n = 3 for all H9 samples); for CTB samples, each dot represents a biological replicate. Clusters from K-means clustering shown in gray dashed circles.

(B) Dendrogram of the same samples, showing primed and naive hPSCs and their early derivatives clustering separately (left) from primary CTB and hPSC-derived TSCs (naive and primed), as well as hPSC-derived TE (naive and primed).

(C) Single-cell RNA-seq analysis of H9-ESCs at day 0, at 12 and 24 h, and at 4 days post BMP4/IWP2 treatment, as well as H9-TSCs, separated into 4 clusters by Seurat. Feature plots of pluripotency-, TE-, and CTB-associated markers show induction of TE- (and not naive pluripotency-) associated genes, prior to finally transitioning into TSC state, with expression of CTB-associated markers.

(D) UCell analysis using epiblast (EPI) and TE-specific genes from single-cell RNA-seq of extended culture human embryo dataset by Zhou et al. (2019). Note clusters 0 (H9-12 and 24 h) and 1 (undifferentiated H9) are enriched in EPI genes, while clusters 2 (H9-TSC) and 3 (H9 at 4 days post BMP4/IWP2 treatment) are enriched in TE genes.

(E) Analysis by PlacentaCellEnrich tool of transcriptomic signatures of BMP4/IWP2-treated hPSCs, primary TSCs, and hPSC-derived TSCs compared with undifferentiated hPSCs. Note similar enrichment proportions for STB-, extravillous trophoblast (EVT)-, and CTB-associated genes across all 3 comparisons.

See also Figure S4.

protocol for obtaining TSCs from a vast array of available embryonic and iPSCs.

DISCUSSION

The modeling of human trophoblast differentiation has proven difficult for multiple reasons, including a significant divergence of factors regulating early embryonic development (Blakeley et al., 2015), as well as the establishment and maintenance of human TSCs (Okae et al., 2018). We previously showed that BMP4-mediated trophoblast differentiation of hPSCs requires TP63 (specifically, the N-terminally truncated isoform ΔN-p63α) (Li et al., 2013), a transcription factor that is widely expressed in stem cells of stratified epithelia, including villous CTB of the human placenta (Lee et al., 2007), and that helps maintain these cells in their undifferentiated state (Haider et al., 2016; Li et al., 2014). Another transcription factor uniquely expressed in human TSCs is VGLL1, a potential co-factor for TEAD4 in this setting (Okae et al., 2018; Saha et al., 2020; Soncin et al., 2018). This contrasts with mouse TSCs, where CDX2 and EOMES play key roles in establishment and/or maintenance (Russ et al., 2000; Strumpf et al., 2005). CDX2 is expressed in human TE and a subset of first-trimester villous CTB (Blakeley et al., 2015; Horii et al., 2016; Soncin et al., 2018); however, its expression is minimal (though variable) in established human TSC lines (Okae et al., 2018), and thus it is unclear whether it in fact plays a role in human TSC maintenance. *EOMES* is completely absent from both human TE and villous CTB at any gestational age (Blakeley et al., 2015; Soncin et al., 2018). Another transcription factor required for mouse TSC maintenance is Elf5 (Donnison et al., 2005). In human, ELF5 is expressed in both villous CTB as well as some cells of the trophoblast column (immature EVT) (Hemberger et al., 2010; Soncin et al., 2018), though its exact role in human TSC establishment and maintenance remains unknown. Further, while it is unclear how closely its expression in human trophoblast is tied to its promoter methylation, that its promoter is hypomethylated in early-gestation trophoblast (particularly compared with undifferentiated hPSCs) has been fully established (Hemberger et al., 2010; Okae et al., 2018). Our hPSC-derived TSCs express all three of these transcription factors (*TP63*, *VGLL1*, and *ELF5*) at similar-to-higher levels than primary placenta-derived TSCs, have a similarly variable expression of CDX2, and show proper hypomethylation of *ELF5* promoter compared with their pluripotent cells of origin. One difference, however, remains with primary hTSC: that is, insufficient upregulation of C19MC miRNAs. It is well known that these miRNAs are maternally imprinted and that their expression tightly regulated by DNA methylation (Noguer-Dance et al., 2010); thus, it is likely that additional manipulation of culture media is required to further enhance their expression in hPSC-derived TSCs. While the high expression of this class of miRNAs is a defining feature of human trophoblast (Donker et al., 2012), their exact role in primary hTSC maintenance and differentiation remains to be explored; therefore, at least for now, the significance of insufficient induction of these miRNAs in hPSC-derived TSCs remains unknown.

Despite this difference in C19MC miRNA expression, our hPSC-derived TSCs fully recapitulate primary TSC function. They are able to differentiate into both hCG-producing STBs and surface HLAG-expressing EVTs. This differentiation potential was recapitulated *in vivo*, by their ability to form trophoblastic tumors in immunocompromised mice, with the typical necrotic center and expression of STB- and EVT-associated markers. Such features of the hPSC-derived TSCs functionally define their true identity as trophoblast and exclude other identities, including amnion. In addition to transcriptomic differences, as described both in our current work and in significantly more detail by Seetharam et al. in this issue of *Stem Cell Reports*, normal amniotic epithelium is a simple cuboidal epithelium, lacking expression of TP63 (Li et al., 2013). Rare reports of amnion expressing HLA-G do not cite specific antibodies used and, in fact, report co-expression of class I HLA molecules in these cells (Strom and Gramignoli, 2016); similarly, the single report of hCG expression in early amnion within the developing human embryo (Xiang et al., 2020) shows staining in a simple, non-stratified epithelium, rather than the secretory ability of a stem cell, following forskolin-induced syncytialization, as occurs in primary TSCs. When morphologic features and marker expression are considered together, hPSC-derived TSCs most closely resemble primary, placenta-derived TSCs and are clearly distinct from amniotic epithelium.

Perhaps the most difficult-to-explain aspect of the trophoblast differentiation ability of primed hPSCs is the developmental trajectory of these cells. The initial segregation of the TE lineage follows the transition from totipotency (2-cell [2C] state) to naive pluripotency, which is the defining feature of pre-implantation inner cell mass (ICM) or EPI (Baker and Pera, 2018; Dong et al., 2019; Rossant and Tam, 2017). It has been suggested that, at least in mouse, this process of lineage segregation into TE and ICM is in fact epigenetically irreversible, precluding mouse ESCs transdifferentiated into TSC-like cells (e.g., by overexpression of *Cdx2*) to significantly contribute to the trophoblast compartment (Cambuli et al., 2014). Primed hPSCs are considered equivalent to post-implantation EPI, a stage of development far beyond TE development, and thus, by definition, should not have the potential to generate TE (De Los Angeles, 2019). In fact, in mouse, both naive and

primed ESCs exclusively give rise to EPI-derived cells when injected into proper stage embryos (Huang et al., 2012; Ying et al., 2008). However, unlike naive mouse ESCs, naive human ESCs have recently been shown by multiple groups to readily give rise to trophoblast (Cinkornpumin et al., 2020; Dong et al., 2020; Guo et al., 2021; Io et al., 2021), suggesting greater plasticity of human ESCs. In addition, it has been shown that media containing BMP4 induces chromatin remodeling in primed mouse ESCs (Kime et al., 2016; Yu et al., 2020), inducing some cells toward a naive, and even 2C-like, fate, while producing TE-like features in other cells (Kime et al., 2019; Tomoda et al., 2021). Our own analysis of primed hPSCs treated with a BMP4-containing medium points to a direct conversion of these cells to a TE-like fate, following 4 days of treatment with BMP4 and IWP2, with induction of only one naive pluripotency marker noted. A comparison with Io et al.'s (2021) naive hPSC-derived cells also showed that primed hPSCs treated with BMP4/IWP2 clustered with naive TE, not naive hPSCs, thus suggesting differentiation into TSCs through a TE intermediate. In addition, a comparison of our scRNA-seq data with that of extended-culture human embryos (Zhou et al., 2019) also showed that BMP4/IWP2-treated primed hPSCs have a gene signature resembling TE, not EPI. Finally, recent reports have shown that direct reprogramming of human fibroblasts to a TSC-like fate can occur when Yamanaka pluripotency factors are applied to the cells, and the medium switched from one used for the culture of hPSCs (embryonic day 7 [E7]) to Okae's TSC medium during reprogramming (Castel et al., 2020). Analysis of the reprogramming process suggests that iTSCs can be captured from a TE-like subpopulation without an initial formation of naive hPSC intermediates (Liu et al., 2020), suggesting perhaps greater plasticity, and fewer epigenetic barriers, between early human stem cell lineages.

Our protocol offers a relatively simple way to convert the many existing hPSC lines, including iPSCs representing many diseases, into TSC-like cells, thus allowing researchers broad access to platforms for human placental research, even where this research may be limited by lack of access to first-trimester placental tissues. Another group has recently published a similar study, showing a role for BMP4 in accelerating the transition of primed hPSCs into TSCs (Wei et al., 2021). Nevertheless, much work, and many questions, remain, including how primed hPSC-derived TSCs compare with similar cells derived from naive hPSCs, not just in their DNA-methylation patterns but in other aspects of their epigenome (including their chromatin and miRNA landscape) as well as their ability to recapitulate trophoblast-based disorders of the placenta. In addition, the different pluripotent states of human ESCs, as well as TE and TSCs, deserve further study in the context of the human embryo, including the extent of their lineage segregation as well as the role of BMP4 in potentially enhancing inter-conversion.

EXPERIMENTAL PROCEDURES

Conversion of hPSC-derived TE to TSC-like cells

Following the first step of trophoblast differentiation from the previously published protocol (Horii et al., 2019) (see also supplemental experimental procedures), hPSC-derived TE-like cells were dissociated using TrypLE Express (Thermo Fisher Scientific) and pelleted by centrifugation at 1,000 RPM for 5 min. hPSC-derived TE-like cells were resuspended in TSC medium and plated with a 1:1 split ratio onto collagen IV- (Millipore Sigma, 5 μg/mL) coated plates. We used a TSC medium that was established in the laboratory of Dr. John Kessler for the optimal growth and passage of primary-term CTB reprogrammed into self-renewing TSC-like cells (Bai et al., 2021), which was composed of Advanced DMEM/F12 (Thermo Fisher Scientific), 1X N2 (Thermo Fisher Scientific), 1X B27 (Thermo Fisher Scientific), 1X Glutmax (Thermo Fisher Scientific), 150 μM 1-thioglycerol (Millipore Sigma), 0.05% BSA (Gemini), 1% knockout serum replacement (KSR; Thermo Fisher Scientific), 2 μM CHIR99021 (Millipore Sigma), 0.5 μM A83-01 (Tocris), 1 μM SB431542 (Millipore Sigma), 5 μM Y27632 (Selleck Chemicals), 130 μg/mL VPA sodium salt (Millipore Sigma), 100 ng/mL recombinant human FGF2 (BioPioneer), 50 ng/mL recombinant human EGF (R&D Systems), 50 ng/mL recombinant human HGF (Stem Cell Technologies), and 20 ng/mL Noggin (R&D System). The medium was replenished every day. Cells were passaged using TrypLE when confluent (approximately every other day) with a split ratio of 1:2 onto collagen IV-coated plates. Conversion into TSC swas deemed complete after at least 5 passages with surface EGFR expression of over 90%, and HLA-G expression of 20% or less, by flow cytometry.

Statistical analysis

All experiments were performed in triplicate. Bar chart data display mean fold change and standard deviation of the mean. Statistical analysis was done using GraphPad Prism 9. Student's t test was performed to determine significance of differences between groups, and the level of significance is represented with an asterisk, as indicated in the figures.

Data and code availability

RNA-seq data have been deposited to the Gene Expression Omnibus database under GEO: GSE182791. The 10 samples of CTB from late first trimester (CTB_1L) were previously deposited in GEO under GEO: GSE173323 (Morey et al., 2021).

SUPPLEMENTAL INFORMATION

Supplemental information can be found online at https://doi.org/10.1016/j.stemcr.2022.04.013.

AUTHOR CONTRIBUTIONS

F.S., R.M., T.B., D.F.R., V.C.C., S.K., R.K., M.G.J., O.F., D.P., and M.H. performed the experiments. M.M. consented patients and

collected samples for this study. F.S., R.M., D.F.R., J.D., and K.M.F. performed the data analysis. F.S., M.H., and M.M.P. designed and supervised the study. F.S., R.M., V.C.C., and M.M.P. wrote the manuscript.

CONFLICTS OF INTERESTS

The authors declare no competing interests.

ACKNOWLEDGMENTS

This work was supported by funds from the National Institutes of Health (NIH)/National Institute of Child Health and Human Development (NICHD) (R01HD-089537 to M.M.P., K99-R00-HD091452 to M.H., and R01-HD096260 to F.S.) and the UC San Diego Stem Cell Program. R.M. and V.C.C. were supported by a grant from the NIH, USA (grant T32GM8806). J.D. was supported by a grant from the American Society for Reproductive Medicine. M.G.J. was supported by the Bridges to Stem Cell Research Internship Program Grant from CIRM (EDUC2-08388). We thank Elsa Molina, PhD, Director of the UC San Diego Stem Cell Genomics & Microscopy Core, for her expert assistance with the scRNA-seq experiments. The manuscript also includes data generated at the UC San Diego IGM Genomics Center utilizing an Illumina NovaSeq 6000 that was purchased with funding from a National Institutes of Health SIG grant (S10 OD026929). The work was also partially supported by NIH grant 2UL1TR001442-06 of CTSA; the content is solely the responsibility of the authors and does not necessarily represent the official views of the NIH. Finally, this publication used the Extreme Science and Engineering Discovery Environment (XSEDE) Comet for computational analysis, which is supported by National Science Foundation grant number ACI-1548562 (allocation ID: TG-MCB140074).

Received: September 1, 2021
Revised: April 18, 2022
Accepted: April 19, 2022
Published: May 19, 2022

REFERENCES

Apps, R., Murphy, S.P., Fernando, R., Gardner, L., Ahad, T., and Moffett, A. (2009). Human leucocyte antigen (HLA) expression of primary trophoblast cells and placental cell lines, determined using single antigen beads to characterize allotype specificities of anti-HLA antibodies. Immunology *127*, 26–39.. https://doi.org/10.1111/j.1365-2567.2008.03019.x.

Armeanu, S., Bitzer, M., Lauer, U.M., Venturelli, S., Pathil, A., Krusch, M., Kaiser, S., Jobst, J., Smirnow, I., Wagner, A., et al. (2005). Natural killer cell–mediated lysis of hepatoma cells via specific induction of NKG2D ligands by the histone deacetylase inhibitor sodium valproate. Cancer Res. *65*, 6321–6329. https://doi.org/10.1158/0008-5472.can-04-4252.

Bai, T., Peng, C.Y., Aneas, I., Sakabe, N., Requena, D.F., Billstrand, C., Nobrega, M., Ober, C., Parast, M., and Kessler, J.A. (2021). Establishment of human induced trophoblast stem-like cells from term villous cytotrophoblasts. Stem Cell Res. *56*, 102507. https://doi.org/10.1016/j.scr.2021.102507.

Baker, C.L., and Pera, M.F. (2018). Capturing totipotent stem cells. Cell Stem Cell *22*, 25–34. https://doi.org/10.1016/j.stem.2017.12.011.

Blakeley, P., Fogarty, N.M.E., del Valle, I., Wamaitha, S.E., Hu, T.X., Elder, K., Snell, P., Christie, L., Robson, P., Niakan, K.K., et al. (2015). Defining the three cell lineages of the human blastocyst by single-cell RNA-seq. Development *142*, 3613. https://doi.org/10.1242/dev.131235.

Burton, G.J., and Jauniaux, E. (2015). What is the placenta? Am. J. Obstet. Gynecol. *213*, S6.e1–S6.e4. https://doi.org/10.1016/j.ajog.2015.07.050.

Cambuli, F., Murray, A., Dean, W., Dudzinska, D., Krueger, F., Andrews, S., Senner, C.E., Cook, S.J., and Hemberger, M. (2014). Epigenetic memory of the first cell fate decision prevents complete ES cell reprogramming into trophoblast. Nat. Commun. *5*, 5538. https://doi.org/10.1038/ncomms6538.

Castel, G., Meistermann, D., Bretin, B., Firmin, J., Blin, J., Loubersac, S., Bruneau, A., Chevolleau, S., Kilens, S., Chariau, C., et al. (2020). Induction of human trophoblast stem cells from somatic cells and pluripotent stem cells. Cell Rep. *33*, 108419. https://doi.org/10.1016/j.celrep.2020.108419.

Cinkornpumin, J.K., Kwon, S.Y., Guo, Y., Hossain, I., Sirois, J., Russett, C.S., Tseng, H.W., Okae, H., Arima, T., Duchaine, T.F., et al. (2020). Naive human embryonic stem cells can give rise to cells with a trophoblast-like transcriptome and methylome. Stem Cell Rep. *15*, 198–213. https://doi.org/10.1016/j.stemcr.2020.06.003.

Dong, C., Fischer, L.A., and Theunissen, T.W. (2019). Recent insights into the naïve state of human pluripotency and its applications. Exp. Cell Res. *385*, 111645. https://doi.org/10.1016/j.yexcr.2019.111645.

Dong, C., Beltcheva, M., Gontarz, P., Zhang, B., Popli, P., Fischer, L.A., Khan, S.A., Park, K.M., Yoon, E.J., Xing, X., et al. (2020). Derivation of trophoblast stem cells from naïve human pluripotent stem cells. Elife *9*, 1–26. https://doi.org/10.7554/elife.52504.

Donker, R.B., Mouillet, J.F., Chu, T., Hubel, C.A., Stolz, D.B., Morelli, A.E., and Sadovsky, Y. (2012). The expression profile of C19MC microRNAs in primary human trophoblast cells and exosomes. Mol. Hum. Reprod. *18*, 417–424. https://doi.org/10.1093/molehr/gas013.

Donnison, M., Beaton, A., Davey, H.W., Broadhurst, R., L'Huillier, P., and Pfeffer, P.L. (2005). Loss of the extraembryonic ectoderm in Elf5 mutants leads to defects in embryonic patterning. Development *132*, 2299–2308. https://doi.org/10.1242/dev.01819.

Guo, G., Stirparo, G.G., Strawbridge, S.E., Spindlow, D., Yang, J., Clarke, J., Dattani, A., Yanagida, A., Li, M.A., Myers, S., et al. (2021). Human naive epiblast cells possess unrestricted lineage potential. Cell Stem Cell *28*, 1040–1056.e6. https://doi.org/10.1016/j.stem.2021.02.025.

Haider, S., Meinhardt, G., Saleh, L., Fiala, C., Pollheimer, J., and Knöfler, M. (2016). Notch1 controls development of the extravillous trophoblast lineage in the human placenta. Proc. Natl. Acad. Sci. U S A *113*, E7710–E7719. https://doi.org/10.1073/pnas.1612335113.

Haider, S., Meinhardt, G., Saleh, L., Kunihs, V., Gamperl, M., Kaindl, U., Ellinger, A., Burkard, T.R., Fiala, C., Pollheimer, J.,

et al. (2018). Self-renewing trophoblast organoids recapitulate the developmental program of the early human placenta. Stem Cell Rep. *11*, 537–551. https://doi.org/10.1016/j.stemcr.2018.07.004.

Hemberger, M., Udayashankar, R., Tesar, P., Moore, H., and Burton, G.J. (2010). ELF5-enforced transcriptional networks define an epigenetically regulated trophoblast stem cell compartment in the human placenta. Hum. Mol. Genet. *19*, 2456–2467. https://doi.org/10.1093/hmg/ddq128.

Horii, M., Li, Y., Wakeland, A.K., Pizzo, D.P., Nelson, K.K., Sabatini, K., Laurent, L.C., Liu, Y., and Parast, M.M. (2016). Human pluripotent stem cells as a model of trophoblast differentiation in both normal development and disease. Proc. Natl. Acad. Sci. U S A *113*, E3882–E3891. https://doi.org/10.1073/pnas.1604747113.

Horii, M., Bui, T., Touma, O., Cho, H.Y., and Parast, M.M. (2019). An improved two-step protocol for trophoblast differentiation of human pluripotent stem cells. Curr. Protoc. Stem Cell Biol. *50*, 1–21. https://doi.org/10.1002/cpsc.96.

Horii, M., Morey, R., Bui, T., Touma, O., Nelson, K.K., Cho, H.Y., Rishik, H., Laurent, L.C., and Parast, M.M. (2021). Modeling preeclampsia using human induced pluripotent stem cells. Sci. Rep. *11*, 5877. https://doi.org/10.1038/s41598-021-85230-5.

Huang, Y., Osorno, R., Tsakiridis, A., and Wilson, V. (2012). In vivo differentiation potential of epiblast stem cells revealed by chimeric embryo formation. Cell Rep. *2*, 1571–1578. https://doi.org/10.1016/j.celrep.2012.10.022.

Io, S., Kabata, M., Iemura, Y., Semi, K., Morone, N., Minagawa, A., Wang, B., Okamoto, I., Nakamura, T., Kojima, Y., et al. (2021). Capturing human trophoblast development with naive pluripotent stem cells in vitro. Cell Stem Cell *28*, 1023–1039.e13. https://doi.org/10.1016/j.stem.2021.03.013.

Jain, A., and Tuteja, G. (2021). PlacentaCellEnrich: a tool to characterize gene sets using placenta cell-specific gene enrichment analysis. Placenta *103*, 164–171. https://doi.org/10.1016/j.placenta.2020.10.029.

Kime, C., Sakaki-Yumoto, M., Goodrich, L., Hayashi, Y., Sami, S., Derynck, R., Asahi, M., Panning, B., Yamanaka, S., and Tomoda, K. (2016). Autotaxin-mediated lipid signaling intersects with LIF and BMP signaling to promote the naive pluripotency transcription factor program. Proc. Natl. Acad. Sci. U S A *113*, 12478–12483. https://doi.org/10.1073/pnas.1608564113.

Kime, C., Kiyonari, H., Ohtsuka, S., Kohbayashi, E., Asahi, M., Yamanaka, S., Takahashi, M., and Tomoda, K. (2019). Induced 2C expression and implantation-competent blastocyst-like cysts from primed pluripotent stem cells. Stem Cell Rep. *13*, 485–498. https://doi.org/10.1016/j.stemcr.2019.07.011.

Kunath, T., Yamanaka, Y., Detmar, J., MacPhee, D., Caniggia, I., Rossant, J., and Jurisicova, A. (2014). Developmental differences in the expression of FGF receptors between human and mouse embryos. Placenta *35*, 1079–1088. https://doi.org/10.1016/j.placenta.2014.09.008.

Kurek, D., Neagu, A., Tastemel, M., Tüysüz, N., Lehmann, J., Van De Werken, H.J.G., Philipsen, S., Van Der Linden, R., Maas, A., Van Ijcken, W.F.J., et al. (2015). Endogenous WNT signals mediate BMP-induced and spontaneous differentiation of epiblast stem cells and human embryonic stem cells. Stem Cell Rep. *4*, 114–128. https://doi.org/10.1016/j.stemcr.2014.11.007.

Lee, Y., Kim, K.R., McKeon, F., Yang, A., Boyd, T.K., Crum, C.P., and Parast, M.M. (2007). A unifying concept of trophoblastic differentiation and malignancy defined by biomarker expression. Hum. Pathol. *38*, 1003–1013. https://doi.org/10.1016/j.humpath.2006.12.012.

Li, Y., Moretto-Zita, M., Soncin, F., Wakeland, A., Wolfe, L., Leon-Garcia, S., Pandian, R., Pizzo, D., Cui, L.L., Nazor, K., et al. (2013). BMP4-directed trophoblast differentiation of human embryonic stem cells is mediated through a ΔNp63+ cytotrophoblast stem cell state. Development *140*, 3965–3976. https://doi.org/10.1242/dev.092155.

Li, Y., Moretto-Zita, M., Leon-Garcia, S., and Parast, M.M. (2014). P63 inhibits extravillous trophoblast migration and maintains cells in a cytotrophoblast stem cell-like state. Am. J. Pathol. *184*, 3332–3343. https://doi.org/10.1016/j.ajpath.2014.08.006.

Liu, X., Ouyang, J.F., Rossello, F.J., Tan, J.P., Davidson, K.C., Valdes, D.S., Schröder, J., Sun, Y.B.Y., Chen, J., Knaupp, A.S., et al. (2020). Reprogramming roadmap reveals route to human induced trophoblast stem cells. Nature *586*, 101–107. https://doi.org/10.1038/s41586-020-2734-6.

De Los Angeles, A. (2019). Frontiers of pluripotency. Methods Mol. Biol. *2005*, 3–27. https://doi.org/10.1007/978-1-4939-9524-0_1.

Mora-García, M. de L., Duenas-González, A., Hernández-Montes, J., De la Cruz-Hernández, E., Pérez-Cárdenas, E., Weiss-Steider, B., Santiago-Osorio, E., Ortíz-Navarrete, V.F., Rosales, V.H., Cantú, D., et al. (2006). Up-regulation of HLA class-I antigen expression and antigen-specific CTL response in cervical cancer cells by the demethylating agent hydralazine and the histone deacetylase inhibitor valproic acid. J. Transl. Med. *4*, 55. https://doi.org/10.1186/1479-5876-4-55.

Morey, R., Farah, O., Kallol, S., Requena, D.F., Meads, M., Moretto-Zita, M., Soncin, F., Laurent, L.C., and Parast, M.M. (2021). Transcriptomic drivers of differentiation, maturation, and polyploidy in human extravillous trophoblast. Front. Cell Dev. Biol. *9*, 702046. https://doi.org/10.3389/fcell.2021.702046.

Niakan, K.K., Han, J., Pedersen, R.A., Simon, C., and Pera, R.A.R. (2012). Human pre-implantation embryo development. Development *139*, 829–841. https://doi.org/10.1242/dev.060426.

Noguer-Dance, M., Abu-Amero, S., Al-Khtib, M., Lefèvre, A., Coullin, P., Moore, G.E., and Cavaillé, J. (2010). The primate-specific microRNA gene cluster (C19MC) is imprinted in the placenta. Hum. Mol. Genet. *19*, 3566–3582. https://doi.org/10.1093/hmg/ddq272.

Okae, H., Toh, H., Sato, T., Hiura, H., Takahashi, S., Shirane, K., Kabayama, Y., Suyama, M., Sasaki, H., and Arima, T. (2018). Derivation of human trophoblast stem cells. Cell Stem Cell *22*, 50–63.e6. https://doi.org/10.1016/j.stem.2017.11.004.

Roost, M.S., Van Iperen, L., Ariyurek, Y., Buermans, H.P., Arindrarto, W., Devalla, H.D., Passier, R., Mummery, C.L., Carlotti, F., De Koning, E.J.P., et al. (2015). KeyGenes, a tool to probe tissue differentiation using a human fetal transcriptional atlas. Stem Cell Rep. *4*, 1112–1124. https://doi.org/10.1016/j.stemcr.2015.05.002.

Rossant, J., and Tam, P.P.L. (2017). New insights into early human development: lessons for stem cell derivation and differentiation. Cell Stem Cell *20*, 18–28. https://doi.org/10.1016/j.stem.2016.12.004.

Russ, A.P., Wattler, S., Colledge, W.H., Aparicio, S.A.J.R., Carlton, M.B.L., Pearce, J.J., Barton, S.C., Surani, M.A., Ryan, K., Nehls, M.C., et al. (2000). Eomesodermin is required for mouse trophoblast development and mesoderm formation. Nature *404*, 95–99. https://doi.org/10.1038/35003601.

Saha, B., Ganguly, A., Home, P., Bhattacharya, B., Ray, S., Ghosh, A., Rumi, M.A.K., Marsh, C., French, V.A., Gunewardena, S., and Paul, S. (2020). TEAD4 ensures postimplantation development by promoting trophoblast self-renewal: an implication in early human pregnancy loss. Proc. Natl. Acad. Sci. U S A *117*, 17864–17875. https://doi.org/10.1073/pnas.2002449117.

Seetharam, A.S., Vu, H.T.H., Choi, S., Khan, T., Sheridan, M.A., Ezashi, T., Roberts, R.M., and Tuteja, G. (2022). The product of BMP-directed differentiation protocols for human primed pluripotent stem cells is placental trophoblast and not amnion. Stem Cell Rep *17*.. https://doi.org/10.1016/j.stemcr.2022.04.014.

Soncin, F., Natale, D., and Parast, M.M. (2015). Signaling pathways in mouse and human trophoblast differentiation: a comparative review. Cell. Mol. Life Sci. *72*, 1291–1302. https://doi.org/10.1007/s00018-014-1794-x.

Soncin, F., Khater, M., To, C., Pizzo, D., Farah, O., Wakeland, A., Rajan, K.A.N., Nelson, K.K., Chang, C.-W., Moretto-Zita, M., et al. (2018). Comparative analysis of mouse and human placentae across gestation reveals species-specific regulators of placental development. Development *145*, dev156273. https://doi.org/10.1242/dev.156273.

Strom, S.C., and Gramignoli, R. (2016). Human amnion epithelial cells expressing HLA-G as novel cell-based treatment for liver disease. Hum. Immunol. *77*, 734–739. https://doi.org/10.1016/j.humimm.2016.07.002.

Strumpf, D., Mao, C.A., Yamanaka, Y., Ralston, A., Chawengsaksophak, K., Beck, F., and Rossant, J. (2005). Cdx2 is required for correct cell fate specification and differentiation of trophectoderm in the mouse blastocyst. Development *132*, 2093–2102. https://doi.org/10.1242/dev.01801.

Tanaka, S., Kunath, T., Hadjantonakis, A.K., Nagy, A., and Rossant, J. (1998). Promotion to trophoblast stem cell proliferation by FGF4. Science *282*, 2072–2075.

Tomoda, K., Hu, H., Sahara, Y., Sanyal, H., Takasato, M., and Kime, C. (2021). Reprogramming epiblast stem cells into pre-implantation blastocyst cell-like cells. Stem Cell Rep. *16*, 1197–1209. https://doi.org/10.1016/j.stemcr.2021.03.016.

Turco, M.Y., Gardner, L., Kay, R.G., Hamilton, R.S., Prater, M., Hollinshead, M.S., McWhinnie, A., Esposito, L., Fernando, R., Skelton, H., et al. (2018). Trophoblast organoids as a model for maternal–fetal interactions during human placentation. Nature *564*, 263–267. https://doi.org/10.1038/s41586-018-0753-3.

Wei, Y., Wang, T., Ma, L., Zhang, Y., Zhao, Y., Lye, K., Xiao, L., Chen, C., Wang, Z., Ma, Y., et al. (2021). Efficient derivation of human trophoblast stem cells from primed pluripotent stem cells. Sci. Adv. *7*, eabf4416. https://doi.org/10.1126/sciadv.abf4416.

Xiang, L., Yin, Y., Zheng, Y., Ma, Y., Li, Y., Zhao, Z., Guo, J., Ai, Z., Niu, Y., Duan, K., et al. (2020). A developmental landscape of 3D-cultured human pre-gastrulation embryos. Nature *577*, 537–542. https://doi.org/10.1038/s41586-019-1875-y.

Yamanegi, K., Yamane, J., Kobayashi, K., Kato-Kogoe, N., Ohyama, H., Nakasho, K., Yamada, N., Hata, M., Nishioka, T., Fukunaga, S., et al. (2010). Sodium valproate, a histone deacetylase inhibitor, augments the expression of cell-surface NKG2D ligands, MICA/B, without increasing their soluble forms to enhance susceptibility of human osteosarcoma cells to NK cell-mediated cytotoxicity. Oncol. Rep. *24*, 1621–1627. https://doi.org/10.3892/or_00001026.

Yang, W., Li, Y., Gao, R., Xiu, Z., and Sun, T. (2020). MHC class I dysfunction of glioma stem cells escapes from CTL-mediated immune response via activation of Wnt/β-catenin signaling pathway. Oncogene *39*, 1098–1111. https://doi.org/10.1038/s41388-019-1045-6.

Ying, Q.L., Wray, J., Nichols, J., Batlle-Morera, L., Doble, B., Woodgett, J., Cohen, P., Smith, A., Johansson, B.M., Wiles, M.V., et al. (2008). The ground state of embryonic stem cell self-renewal. Nature *453*, 519–523. https://doi.org/10.1038/nature06968.

Yu, S., Zhou, C., Cao, S., He, J., Cai, B., Wu, K., Qin, Y., Huang, X., Xiao, L., Ye, J., et al. (2020). BMP4 resets mouse epiblast stem cells to naive pluripotency through ZBTB7A/B-mediated chromatin remodelling. Nat. Cell Biol. *22*, 651–662. https://doi.org/10.1038/s41556-020-0516-x.

Zhou, F., Wang, R., Yuan, P., Ren, Y., Mao, Y., Li, R., Lian, Y., Li, J., Wen, L., Yan, L., et al. (2019). Reconstituting the transcriptome and DNA methylome landscapes of human implantation. Nature *572*, 660–664. https://doi.org/10.1038/s41586-019-1500-0.